Simulating the Initial Stage of Phenolic Resin Carbonization via the ReaxFF Reactive Force Field

De-en Jiang,*,† Adri C. T. van Duin,‡ William A. Goddard III,§ and Sheng Dai†

Chemical Sciences Division, Oak Ridge National Laboratory, Oak Ridge, Tennessee 37831, Department of Mechanical and Nuclear Engineering, The Pennsylvania State University, 136 Research Building East, University Park, Pennsylvania 16802, and Materials and Process Simulation Center, Division of Chemistry and Chemical Engineering, California Institute of Technology, Pasadena, California 91125

Received: April 1, 2009; Revised Manuscript Received: May 7, 2009

Pyrolysis of phenolic resins leads to carbon formation. Simulating this resin-to-carbon process atomistically is a daunting task. In this paper, we attempt to model the initial stage of this process by using the ReaxFF reactive force field, which bridges quantum mechanical and molecular mechanical methods. We run molecular dynamics simulations to examine the evolution of small molecules at different temperatures. The main small-molecule products found include H_2O, H_2, CO, and C_2H_2. We find multiple pathways leading to H_2O formation, including a frequent channel via β-H elimination, which has not been proposed before. We determine the reaction barrier for H_2O formation from the reaction rates obtained at different temperatures. We also discuss the relevance of our simulations to previous experimental observations. This work represents a first attempt to model the resin-to-carbon process atomistically.

1. Introduction

Phenolic resins are a good source of carbon. Direct pyrolysis of neat phenolic resins can lead to glassy carbons[1] and microporous activated carbons.[2] Phenolic resins are also used as a carbon source to make carbon/carbon composite materials.[3] Recently, the soft-template synthesis of mesoporous carbons was developed[4−6] in which phenolic resins are formed in the hydrophilic region of the micelles of the block-copolymer template. Subsequent heat treatment results in the formation of porous carbons: the phenolic resin region turns into carbon walls, while the hydrophobic region of the template decomposes into empty space. The soft-template synthesis of porous carbons allows better control of the pore sizes and morphology than the traditional way of making activated carbons.[6]

The resin-to-carbon process is a complicated process and even more complicated in the soft-template synthesis of mesoporous carbons because of the additional complexity due to the block-copolymer template. Modeling this process atomistically is challenging. Because chemical reactions are constantly happening during a carbonization process, one needs to employ a simulation method that can handle dynamic bond breaking and formation. Although quantum chemical methods are a natural choice for studying chemical reactions, they are prohibitively expensive to apply to the resin-to-carbon process, which requires a simulation cell consisting of at least several hundred atoms. Previously, semiempirical methods such as tight-binding and extended Hückel methods have been applied to study structures of porous carbons,[7] but they are probably also too expensive to apply to the resin-to-carbon process. Recently, Kumar et al. used Monte Carlo simulations to create structural models for porous carbons based on the amorphous polyfurfuryl polymer.[8] Although the resultant models display properties in good agreement with the experiment, we note that the non-carbon atoms (oxygen and hydrogen) had to be artificially removed from the polymer chain before it was fed into the Monte Carlo simulations.

Bridging the time and length scales of quantum chemical and molecular mechanical methods, the reactive force field (ReaxFF) was developed by van Duin et al.[9] ReaxFF employs a relationship between bond orders and bond lengths and allows smooth bond forming and breaking. This method has been quite successfully applied to a variety of chemical problems,[10−22] including thermal degradation of polymers.[12] Even with the ReaxFF method, the time scale accessible for routine molecular dynamics simulations is currently limited to the subnanosecond range, which at least allows us to study the initial stage of resin carbonization. Massive parallelization of the ReaxFF method is expected to dramatically increase the accessible time scale.[23]

In this paper, we apply the ReaxFF method to the initial stage of the resin-to-carbon process. Our goal is to find out the major reaction products and the pathways leading to their formation. By examining product evolution at different temperatures, we also seek to obtain the kinetics of the initial pyrolysis process. The rest of the paper is organized as follows: Section 2 describes the ReaxFF method and simulation details; section 3 shows simulation results and analysis for temperature ramping and constant-temperature runs and discusses implications for experiments; section 4 summarizes and concludes our findings.

2. Method

The ReaxFF program developed by van Duin et al.[9] was used to perform ReaxFF simulations. ReaxFF parameters for carbon, hydrogen, and oxygen were taken from a previously optimized data set.[17] A total of 16 phenolic resin polymeric chains were placed in parallel along the *y* direction in a box of 3 nm × 3 nm × 3 nm, giving an initial density of 0.70 g/cm^3. Then the system was energy-minimized to a force tolerance of 1 kcal/mol/Å. The dimensions of the box were gradually scaled down to 2.52 nm × 2.83 nm × 2.52 nm to achieve a typical experimental resin density of 1.25 g/cm^3. The system then was

* To whom correspondence should be addressed. E-mail: jiangd@ornl.gov. Phone: (865) 574-5199. Fax: (865) 576-5235.
† Oak Ridge National Laboratory.
‡ The Pennsylvania State University.
§ California Institute of Technology.

10.1021/jp902986u CCC: $40.75
Published on Web 06/04/2009

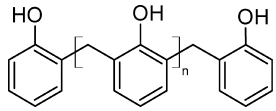

Figure 1. Polymeric chain of a non-cross-linked phenol formaldehyde resin.

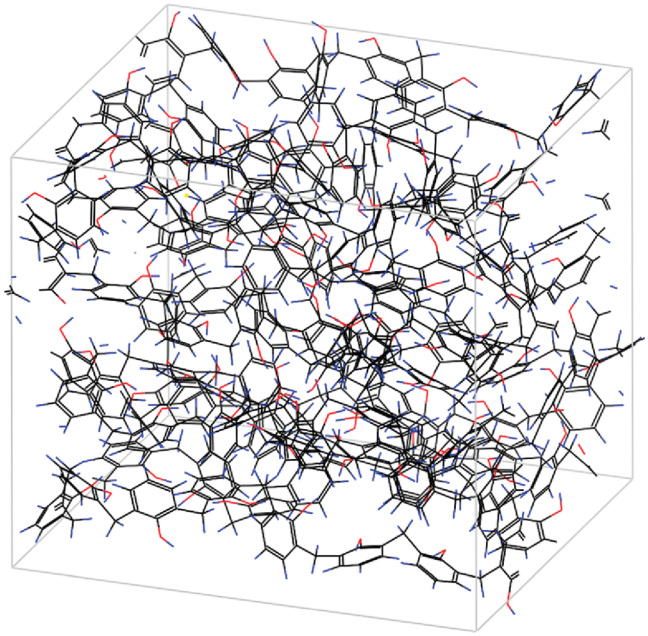

Figure 2. Snapshot of the simulation cell equilibrated at 300 K. The cell consists of 16 chains of a phenol formaldehyde resin polymer. Color code: C, black; O, red; H, blue.

equilibrated at 300 K with an NVT-MD simulation for 10 ps with a time step of 0.25 fs and a temperature damping constant of 100 fs. In a temperature-ramping simulation, the equilibrated system was heated at a rate of 0.08 K/fs to 4000 K. NVT-MD simulations were also performed at 2750, 2875, 3000, 3125, and 3250 K for 20 ps to obtain reaction rates.

3. Results and Discussion

We consider here the non-cross-linked phenolic formaldehyde resin, as shown in Figure 1. A total of 16 such polymeric chains, each consisting of five repeating units, are included a simulation box, to model a unit cell of the condensed-phase resin. Figure 2 shows the resin at a density of 1.25 g/cm^3 after equilibrating at 300 K for 10 ps. We then heated the system to 4000 K to find the temperature at which small-molecule products begin to form (Figure 3). We found that H_2O formation happens first when the temperature reaches ~2900 K, followed by formation of H_2 and C_2H_2. CO formation begins at ~3600 K. At 4000 K, major products from the cookoff simulation include H_2O, H_2, C_2H_2, and CO.

Table 1 shows all of the reaction products at the end of the cookoff simulation (Figure 3). The largest fragment has a molecular weight about 8 times that of the original single-chain segment ($C_{56}H_{48}O_8$, molecular weight = 848.4) and results from the cross-linking of individual chains. The fragments with 10−50 carbon atoms result from a breaking down of the individual chains. The original resin has a stoichiometry of C_7H_6O, while that of the largest fragment from Table 1 is $C_{11.5}H_{8.1}O$, leading to an increase in both C/H and C/O ratios after the cookoff. This simulation indicates that formation of H_2O and H_2 is an effective way to decrease the hydrogen and oxygen contents.

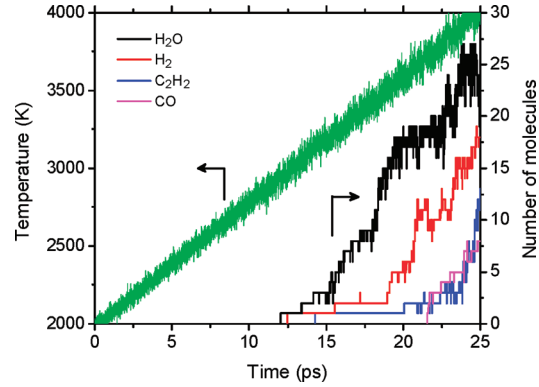

Figure 3. Evolution of small-molecule products with time during temperature ramping from 2000 to 4000 K.

TABLE 1: Products Formed after Temperature Ramping to 4000 K

molecular formula	no. of molecules	molecular formula	no. of molecules
$C_{447}H_{316}O_{39}$	1	C_4H_4	1
$C_{88}H_{67}O_{13}$	1	C_2H_4O	1
$C_{72}H_{53}O_8$	1	C_2H_3O	2
$C_{49}H_{39}O_5$	1	C_2H_2O	2
$C_{34}H_{31}O_5$	1	C_2HO	1
$C_{34}H_{25}O_3$	1	CH_2O	2
$C_{20}H_{14}O_2$	1	C_2H_4	1
$C_{16}H_{13}O_3$	1	CO	8
$C_{16}H_{14}O$	1	C_2H_3	2
$C_{12}H_{11}O_2$	1	C_2H_2	13
$C_8H_7O_3$	1	C_2H	4
C_9H_7O	1	H_2O	22
C_8H_7	1	HO	1
C_7H_6	1	CH_3	2
$C_2H_2O_2$	1	H_2	18
C_3H_3O	2		

Because H_2O is found here to be the first reaction product, we examined in detail the mechanisms for its formation. We analyzed nine events of H_2O formation for a 20-ps NVT-MD run at 3000 K. We found three occurrences of β-hydrogen elimination, as shown in Figure 4. This mechanism is found to happen quite frequently in our simulations. We also see two occurrences of intermolecular dehydration from one −OH group and one hydrogen atom in the $-CH_2-$ group (Figure 5). Moreover, we found two occurrences of intermolecular dehydration between two −OH groups, one occurrence of dissociated hydrogen extracting an −OH group, and one occurrence of intermolecular dehydration between a hydrogen atom attached to a carbon ring and one −OH group. These observations indicate multiple channels for H_2O formation.

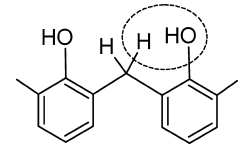

Figure 4. β-hydrogen elimination mechanism of H_2O formation.

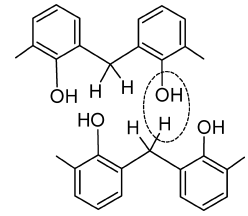

Figure 5. Interchain dehydration mechanism from −OH and $-CH_2-$.

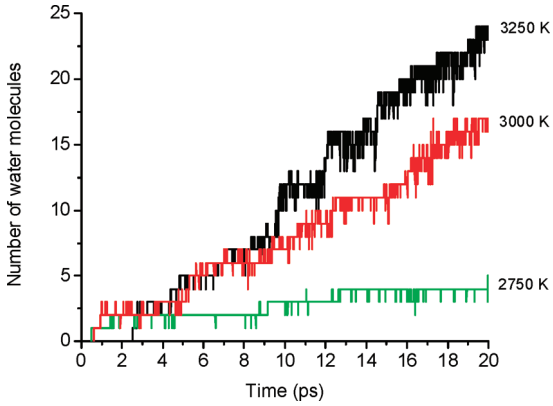

Figure 6. Evolution of H_2O with time at temperatures from 2750 to 3250 K.

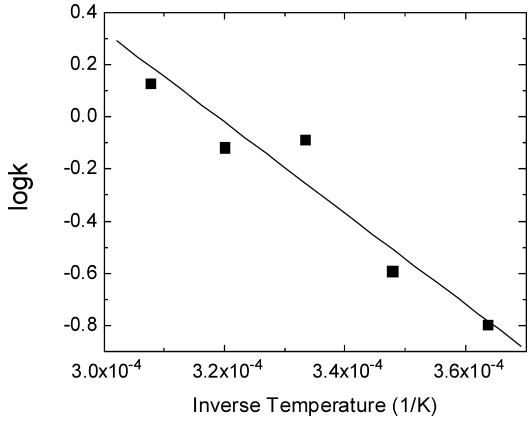

Figure 7. Logarithm of the H_2O formation rate (K) versus the inverse temperature.

H_2O evolution from pyrolysis of the phenolic resin has been observed by mass spectrometry[24] and proposed to be a major reaction responsible for cross-linking of resin chains.[1,24] Although intermolecular condensation between two −OH groups or between methylene and −OH groups has been suggested before[1,24] and confirmed in this work, H_2O formation by β-hydrogen elimination observed in our simulation is new. Our simulation indicates two roles for this new mechanism in the resin-to-carbon process: (a) it converts the sp^3 methylene carbon to a sp^2 carbon; (b) it creates an unsaturated valence on the carbon ring, which will readily react with neighboring groups.

We next investigated the rate of H_2O formation at different temperatures. Figure 6 displays H_2O evolution during a 20-ps NVT-MD run for temperatures between 2750 and 3250 K. One can see that the rate of H_2O formation (that is, the slope) increases with the temperature. From a least-squares fit of the data sets (including temperatures at 2875 and 3125 K, which are not shown in Figure 6), we derived the rate of H_2O formation for each temperature and plotted them in Figure 7. Using the Arrhenius equation, we obtained a reaction barrier of 144 ± 28 kJ/mol for H_2O formation. Trick and Saliba studied the pyrolysis kinetics of the phenolic resin in a carbon/phenolic composite via thermogravimetric analysis and obtained apparent activation energies ranging from 74 to 199 kJ/mol for four mass-loss peaks.[3] Our computed barrier is within this experimental range.

Because the β-hydrogen elimination is found to be the most frequent mechanism for H_2O formation in our simulations, there may be a close relationship between the barrier for the β-hydrogen elimination and that from the Arrhenius equation (Figure 7). To test this hypothesis, we used the ReaxFF program

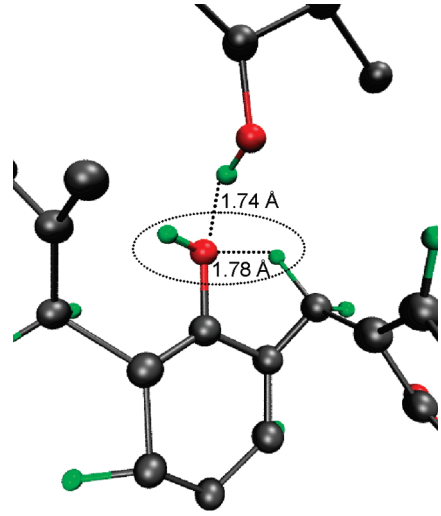

Figure 8. Approximate transition state of the β-hydrogen elimination mechanism of H_2O formation during a molecular dynamics simulation. The circle indicates H_2O formation, and the dotted lines indicate O−H interactions. Color code: C, gray; O, red; H, green.

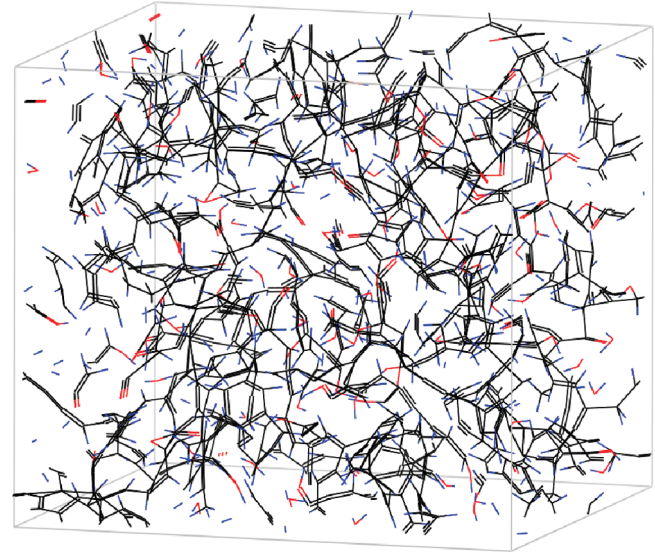

Figure 9. Snapshot of the simulated system after a 20-ps NVT-MD run at 3500 K. Color code: C, black; O, red; H, blue.

to search the transition state for the β-hydrogen elimination of an isolated phenolic resin fragment (as shown in Figure 4). We found a barrier of 230 kJ/mol, much higher than the one from the condensed-phase simulation (Figure 7). This indicates a significant role from the surrounding environment on the barrier and prompted us to examine closely the β-hydrogen elimination mechanism of H_2O formation in the condensed-phase molecular dynamics simulations. We indeed found that in several cases a nearby −OH group stabilizes the transition state of the β-hydrogen elimination, as shown in Figure 8, thereby lowering the reaction barrier.

Although the time-scale limitation still prevents us from observing larger graphene fragments [which are observed by high-resolution transmission electron microscopy (TEM) to be building blocks for glassy carbon from resin[25,26]], we do find small fused rings and five- and seven-membered rings after a short (~20 ps) run of the molecular dynamics simulation. Figure 9 displays a snapshot for the system after a 20-ps NVT-MD run at 3500 K. From this snapshot, we identified a fused ring, as shown in Figure 10. This small patch can serve as a seed for

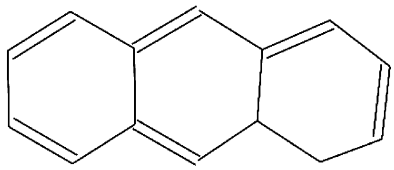

Figure 10. Fused-ring fragment from a 20-ps NVT-MD run at 3500 K.

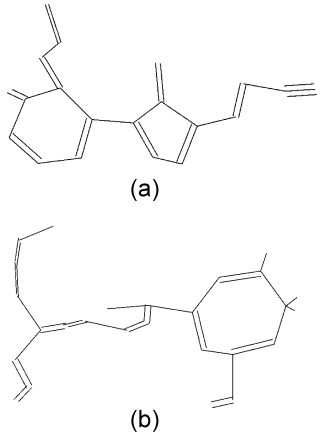

Figure 11. Fragments with five- (a) and seven-membered (b) rings from a 20-ps NVT-MD run at 3500 K.

the formation of large graphene fragments. We also identified five- and seven-membered rings (Figure 11).

Experimental carbonization of phenolic resins usually takes places under an inert atmosphere at a low (~1300 K) or high (~3300 K) temperature.[25] High-resolution TEM images show that the high-temperature treatment leads to fullerene-related nanostructures and enclosed spaces in the glassy carbon.[25,26] Although our simulation does show many reactions happening at 3250 K, large patches of graphene- or fullerene-related structures are not observed. There are reasons for this. First, limited by the time-scale problem in all molecular dynamics methods,[27] our simulation time frame is relatively short (~20 ps) because we used high temperatures to accelerate the chemical reactions that would take a prohibitively long simulation time to happen at a lower temperature (for example, at 1000 K). We hope that massive parallelization of the ReaxFF program can propel the simulation into the microsecond regime, so large patches of graphenes could be observed and lower simulation temperatures could be used. Second, we performed the simulations in an NVT ensemble, where the simulated system is closed, while experiments are usually conducted under a continuous gas flow, which takes away pyrolysis products. The implementation of the grand canonical ensemble (which is not available in the current ReaxFF program) may help bring our simulations closer to the real world by allowing exchanges of chemical species between our simulated system and the reservoirs.

Depending on the precursor, the carbon formed can be a graphitizing or nongraphitizing one.[26] The present work focused on the nongraphitizing carbon formed from pyrolysis of a phenolic resin polymer, motivated by our experimental research of porous, nongraphitizing carbons.[6] Certainly, using ReaxFF to model the process of forming a graphitizing carbon (such as from anthracene[26]) would be very interesting and make a good comparison with the nongraphitizing case.

4. Summary and Conclusions

Using ReaxFF, we modeled the initial process of resin carbonization. We found H_2O formation to be the first reaction to occur. Other small-molecule products observed in our simulation include H_2, CO, and C_2H_2. We found several pathways for H_2O formation, and the most frequent turned out to be β-hydrogen elimination, which has not been proposed before. H_2O formation is found to have a reaction barrier of 144 ± 28 kJ/mol, which is within the experimental range. Our simulation here represents a first attempt to model the initial chemical events of resin carbonization and provides a significant step toward our goal to model atomistically the resin-to-carbon process.

Acknowledgment. The work was supported by Office of Basic Energy Sciences, U.S. Department of Energy, under Contract DE-AC05-00OR22725 with UT-Battelle, LLC.

References and Notes

(1) Jenkins, G. M.; Kawamura, K.; Ban, L. L. *Proc. R. Soc. London, Ser. A* **1972**, *327*, 501.
(2) Tennison, S. R. *Appl. Catal., A* **1998**, *173*, 289.
(3) Trick, K. A.; Saliba, T. E. *Carbon* **1995**, *33*, 1509.
(4) Liang, C. D.; Hong, K. L.; Guiochon, G. A.; Mays, J. W.; Dai, S. *Angew. Chem., Int. Ed.* **2004**, *43*, 5785.
(5) Liang, C. D.; Dai, S. *J. Am. Chem. Soc.* **2006**, *128*, 5316.
(6) Liang, C.; Li, Z.; Dai, S. *Angew. Chem., Int. Ed.* **2008**, *47*, 3696.
(7) Bandosz, T. J.; Biggs, M. J.; Gubbins, K. E.; Hattori, Y.; Iiyama, T.; Kaneko, K.; Pikunic, J.; Thomson, K. T. Molecular models of porous carbons. In *Chemistry and Physics of Carbon*; Radovic, L. R., Ed.; Marcel Dekker: New York, 2003; p 41.
(8) Kumar, A.; Lobo, R. F.; Wagner, N. J. *Carbon* **2005**, *43*, 3099.
(9) van Duin, A. C. T.; Dasgupta, S.; Lorant, F.; Goddard, W. A. *J. Phys. Chem. A* **2001**, *105*, 9396.
(10) Strachan, A.; van Duin, A. C. T.; Chakraborty, D.; Dasgupta, S.; Goddard, W. A. *Phys. Rev. Lett.* **2003**, *91*, 098301.
(11) van Duin, A. C. T.; Strachan, A.; Stewman, S.; Zhang, Q. S.; Xu, X.; Goddard, W. A. *J. Phys. Chem. A* **2003**, *107*, 3803.
(12) Chenoweth, K.; Cheung, S.; van Duin, A. C. T.; Goddard, W. A.; Kober, E. M. *J. Am. Chem. Soc.* **2005**, *127*, 7192.
(13) Nielson, K. D.; van Duin, A. C. T.; Oxgaard, J.; Deng, W. Q.; Goddard, W. A. *J. Phys. Chem. A* **2005**, *109*, 493.
(14) van Duin, A. C. T.; Zeiri, Y.; Dubnikova, F.; Kosloff, R.; Goddard, W. A. *J. Am. Chem. Soc.* **2005**, *127*, 11053.
(15) Buehler, M. J.; van Duin, A. C. T.; Goddard, W. A. *Phys. Rev. Lett.* **2006**, *96*, 095505.
(16) Goddard, W. A.; van Duin, A.; Chenoweth, K.; Cheng, M. J.; Pudar, S.; Oxgaard, J.; Merinov, B.; Jang, Y. H.; Persson, P. *Top. Catal.* **2006**, *38*, 93.
(17) Chenoweth, K.; van Duin, A. C. T.; Goddard, W. A. *J. Phys. Chem. A* **2008**, *112*, 1040.
(18) Chenoweth, K.; van Duin, A. C. T.; Persson, P.; Cheng, M. J.; Oxgaard, J.; Goddard, W. A. *J. Phys. Chem. C* **2008**, *112*, 14645.
(19) Sanz-Navarro, C. F.; Astrand, P. O.; Chen, D.; Ronning, M.; van Duin, A. C. T.; Mueller, J. E.; Goddard, W. A. *J. Phys. Chem. C* **2008**, *112*, 12663.
(20) van Duin, A. C. T.; Merinov, B. V.; Han, S. S.; Dorso, C. O.; Goddard, W. A. *J. Phys. Chem. A* **2008**, *112*, 11414.
(21) van Duin, A. C. T.; Merinov, B. V.; Jang, S. S.; Goddard, W. A. *J. Phys. Chem. A* **2008**, *112*, 3133.
(22) Zhu, R.; Janetzko, F.; Zhang, Y.; van Duin, A. C. T.; Goddard, W. A.; Salahub, D. R. *Theor. Chem. Acc.* **2008**, *120*, 479.
(23) Nomura, K. I.; Kalia, R. K.; Nakano, A.; Vashishta, P.; van Duin, A. C. T.; Goddard, W. A. *Phys. Rev. Lett.* **2007**, *99*, 148303.
(24) Yamashita, Y.; Ouchi, K. *Carbon* **1981**, *19*, 89.
(25) Harris, P. J. F. *Philos. Mag.* **2004**, *84*, 3159.
(26) Harris, P. J. F. *Crit. Rev. Solid State Mater. Sci.* **2005**, *30*, 235.
(27) Chan, H. S.; Dill, K. A. *Phys. Today* **1993**, *46*, 24.

JP902986U